ISSN 1674-1056
http://cpb.iphy.ac.cn
http://iopscience.iop.org/cpb
中国物理 B
Chinese Physics
中国物理
Chinese Physics B

Further analysis of scintillation index for a laser beam propagating through moderate-to-strong non-Kolmogorov turbulence based on generalized effective atmospheric spectral model

Jing Ma(马晶), Yu-Long Fu(付玉龙), Si-Yuan Yu(于思源), Xiao-Long Xie(谢小龙), Li-Ying Tan(谭立英)
Citation: Chin. Phys. B . 2018, 27(3): 034201. **doi:** 10.1088/1674-1056/27/3/034201

Journal homepage: http://cpb.iphy.ac.cn; http://iopscience.iop.org/cpb

What follows is a list of articles you may be interested in

Quantum polarization fluctuations of partially coherent dark hollow beams in non-Kolmogorov turbulence atmosphere

Xiang Yan(闫香), Peng-Fei Zhang(张鹏飞), Jing-Hui Zhang(张京会), Chun-Hong Qiao(乔春红), Cheng-Yu Fan(范承玉)
Chin. Phys. B . 2016, 25(8): 084204. **doi:** 10.1088/1674-1056/25/8/084204

Estimation of random errors for lidar based on noise scale factor

Wang Huan-Xue, Liu Jian-Guo, Zhang Tian-Shu
Chin. Phys. B . 2015, 24(8): 084213. **doi:** 10.1088/1674-1056/24/8/084213

Scattering of a general partially coherent beam from a diffuse target in atmospheric turbulence

Wang Li-Guo, Wu Zhen-Sen, Wang Ming-Jun, Cao Yun-Hua, Zhang Geng
Chin. Phys. B . 2014, 23(9): 094202. **doi:** 10.1088/1674-1056/23/9/094202

A further study on the spreading and directionality of Gaussian array beams in non-Kolmogorov turbulence

Lu Lu, Ji Xiao-Ling, Deng Jin-Ping, Li Xiao-Qing
Chin. Phys. B . 2014, 23(6): 064209. **doi:** 10.1088/1674-1056/23/6/064209

Measurements of NO_2 mixing ratios with topographic target light scattering-differential optical absorption spectroscopy system and comparisons to point monitoring technique

Wang Yang, Li Ang, Xie Pin-Hua, Zeng Yi, Wang Rui-Bin, Chen Hao, Pei Xian, Liu Jian-Guo, and Liu Wen-Qing
Chin. Phys. B . 2012, 21(11): 114211. **doi:** 10.1088/1674-1056/21/11/114211

Further analysis of scintillation index for a laser beam propagating through moderate-to-strong non-Kolmogorov turbulence based on generalized effective atmospheric spectral model

Jing Ma(马晶), Yu-Long Fu(付玉龙)†, Si-Yuan Yu(于思源), Xiao-Long Xie(谢小龙), and Li-Ying Tan(谭立英)

National Key Laboratory of Tunable Laser Technology, Harbin Institute of Technology, Harbin 150001, *China*

(Received 29 September 2017; revised manuscript received 30 November 2017; published online 13 February 2018)

A new expression of the scintillation index (SI) for a Gaussian-beam wave propagating through moderate-to-strong non-Kolmogorov turbulence is derived, using a generalized effective atmospheric spectrum and the extended Rytov approximation theory. Finite inner and outer scale parameters and high wave number "bump" are considered in the spectrum with a generalized spectral power law in the range of 3–4, instead of the fixed classical Kolmogorov power law of 11/3. The obtained SI expression is then used to analyze the effects of the spectral power law and the inner scale and outer scale on SI under various non-Kolmogorov fluctuation conditions. These results will be useful in future investigations of optical wave propagation through atmospheric turbulence.

Keywords: atmospheric optics, non-Kolmogorov turbulence, scintillation index, Gaussian-beam wave

PACS: 42.25.Bs, 42.25.Dd, 42.68.Bz, 42.68.Ay **DOI:** 10.1088/1674-1056/27/3/034201

1. Introduction

Recently, free space optical (FSO) communication has attracted considerable attention owing to its unique advantages compared with radio communication, such as a large bandwidth, high data transfer rate, license-free usage, and good confidentiality.[1,2] However, FSO communication is subject to many challenges. One of the major difficulties is atmospheric turbulence, which results in irradiance scintillation and beam wander. In particular, irradiance scintillation can degrade the performance of FSO systems. For a long time, the Kolmogorov power spectrums were extensively used to describe atmospheric turbulence.[3–7] However, recent experimental data[8–10] indicated that the turbulence in the upper troposphere and stratosphere layers deviate from the Kolmogorov model. In addition, theoretical investigations[11,12] have also shown that the Kolmogorov spectrum is not the only possible turbulence in the atmosphere. This prompted investigations of optical wave propagation through the more general non-Kolmogorov turbulence.

To model the non-Kolmogorov characteristics of upper atmospheric turbulence, several power spectrums have been proposed, such as the generalized Kolmogorov spectrum,[13] the generalized von Karman spectrum,[14] the generalized effective atmospheric spectrum,[15,16] the generalized modified atmospheric spectrum[16] and so on. Based on these spectra, many theoretical works have been conducted to study the irradiance scintillation for the plane and spherical waves.[13,15,17–19] However, in many applications, these waves are not sufficient to describe the propagation properties of a laser beam.[20] Therefore, a detailed investigation of the propagation properties of a Gaussian-beam wave propagation through non-Kolmogorov atmospheric turbulence is important and necessary. In Refs. [21] and [22] the expressions of the scintillation index (SI) of a such a beam propagating through weak non-Kolmogorov turbulence was investigated based on the generalized Kolmogorov spectrum. However, because this spectral model does not consider the effects of finite inner and outer scales and the high wave number "bump", in Refs. [23] and [24], the irradiance scintillation for a Gaussian-beam wave propagating through weak non-Kolmogorov turbulence using the generalized von Karman spectrum and generalized modified atmospheric spectrum have been analyzed, respectively. Under moderate-to-strong non-Kolmogorov turbulence, when ignoring the effects of inner and outer scales, the expressions of the SI of a Gaussian beam wave in moderate-to-strong turbulence have been developed for a point receiver in Ref. [20] and for an aperture-averaging receiver in Ref. [25] by exploiting the extended Rytov approximation theory. However, previous work on the SI of a Gaussian beam has a few limitations. In particular, the high wave number "bump" and the finite inner and outer scales are not all considered in moderate-to-strong non-Kolmogorov turbulence. In fact, the "bump" at the high wave number is clearly revealed in the experimental data,[26,27] and the outer scale is usually assumed to increase linearly with the order of the height above ground level of the observation point, in the surface layer up to about 100 m.[3,28] The inner scale is typically of the order of 1–10 mm near the ground and of the order of centimeters or more in the upper

†Corresponding author. E-mail: fuyulongm@163.com

© 2018 Chinese Physical Society and IOP Publishing Ltd

atmosphere.[3] Therefore, it is important to investigate the SI of a Gaussian-beam wave propagating through moderate-to-strong non-Kolmogorov atmospheric turbulence, while also considering the high wave number "bump" and the inner and outer scale effects. Although, Kolmogorov turbulence can be regarded as a special case of the non-Kolmogorov turbulence, the results derived for Kolmogorov turbulence[4] cannot be applied directly to the non-Kolmogorov turbulence case.[17] To the best of our knowledge, the effects of inner and outer scales on SI are less clear for a Gaussian-beam wave propagating through moderate-to-strong non-Kolmogorov atmospheric turbulence. This is one of the primary considerations which motivates this work.

Based on the aforesaid discussions, the contributions of this paper are summarized as follows: by using the extended Rytov approximation theory and the generalized effective atmospheric spectrum, which includes finite turbulence inner and outer scales and high wave number "bump", the SI for a Gaussian-beam wave propagating through moderate-to-strong non-Kolmogorov turbulence is derived. Analytic expressions are obtained, which are more general compared to previous results. The expressions are then used to analyze the effects of inner scale, outer scale, path length, and spectral power law on SI.

The following sections of the paper are organized as follows. In Section 2, we introduce the generalized effective atmospheric spectrum. In Section 3, we present the expressions of irradiance scintillation for a Gaussian-beam wave in non-Kolmogorov turbulence. In Section 4, we provide numerical results to analyze the effects of inner scale, outer scale and the spectral power law on SI. Finally, conclusions are given in Section 5.

2. Generalized effective atmospheric spectrum

In this paper, the generalized effective atmospheric spectrum model is used to describe the moderate-to-strong non-Kolmogorov turbulence. This model includes finite turbulence inner and outer scales and high wave number "bump", and has a generalized spectral power law value in the range of 3–4, instead of the fixed classical Kolmogorov power law value of 11/3. It has the following form:[15,16]

$$\begin{aligned}\Phi_{n,\mathrm{eff}}(\kappa,\alpha) &= \Phi_n(\kappa,\alpha)G(\kappa,\alpha,l_0,L_0),\\ &\quad(0\le\kappa<\infty,3<\alpha<4),\end{aligned}\tag{1}$$

where $\Phi_n(\kappa,\alpha)$ is the spectral model for weak non-Kolmogorov turbulence and is given by[13]

$$\Phi_n(\kappa,\alpha)=A(\alpha)\tilde{C}_n^2\kappa^{-\alpha},\quad(0\le\kappa<\infty,3<\alpha<4),\tag{2}$$

where κ is the magnitude of the three-dimensional wave number vector with units of rad/m and is related to the size of the turbulence cells, α is the spectral power law exponent, $A(\alpha)=\cos(\alpha\pi/2)\Gamma(\alpha-1)/(4\pi^2)$, L_0 and l_0 are the turbulence outer scale and inner scale, respectively, $\Gamma(\cdot)$ is the gamma function, and $\tilde{C}_n^2$ is the generalized refractive-index structure constant with units of $\mathrm{m}^{3-\alpha}$. When $\alpha=11/3$, $\tilde{C}_n^2$ reduces to the known structure constant of the Kolmogorov turbulence C_n^2 with units of $\mathrm{m}^{-2/3}$. Moreover, the equivalence of the structure constants in non-Kolmogorov and Kolmogorov spectra in a turbulent atmosphere has been derived[29] and is as follows:

$$\begin{aligned}\tilde{C}_n^2 &= -\frac{\Gamma(\alpha)(k/L)^{\alpha/2-11/6}}{8\pi^2\Gamma(1-\alpha/2)\Gamma^2(\alpha/2)\sin(\pi\alpha/4)A(\alpha)}C_n^2\\ &= h(\alpha)C_n^2,\end{aligned}\tag{3}$$

where $k=2\pi/\lambda$ is the optical wave number, λ is the wavelength, and L is the path length of the optical link.

In Eq. (1), $G(\kappa,\alpha,l_0,L_0)$ is the amplitude spatial filter function and given by

$$G(\kappa,\alpha,l_0,L_0)=G_X(\kappa,\alpha,l_0,L_0)+G_Y(\kappa,\alpha,l_0),\tag{4}$$

where $G_X(\kappa,\alpha,l_0,L_0)$ and $G_Y(\kappa,\alpha,L_0)$ are the large-scale and small-scale filter functions, respectively. Since the inner and outer scales must be taken into account, the filter functions are given by[3]

$$G_X(\kappa,\alpha,l_0,L_0)=f(\kappa,\alpha,l_0)g(\kappa,\alpha,L_0)\exp\left[-\frac{\kappa^2}{\kappa_X^2(\alpha)}\right],\tag{5}$$

$$G_Y(\kappa,\alpha,l_0)=\frac{\kappa^\alpha}{\left[\kappa^2+\kappa_Y^2(\alpha)\right]^{\alpha/2}}\exp\left[\frac{\Lambda L\kappa^2(1-z/L)^2}{k}\right],\tag{6}$$

with

$$\begin{aligned}f(\kappa,\alpha,l_0)&=\left[1+a_1\left(\frac{\kappa}{\kappa_l}\right)-b_1\left(\frac{\kappa}{\kappa_l}\right)^\beta\right]\exp\left(-\frac{\kappa^2}{\kappa_l^2}\right),\\ g(\kappa,\alpha,L_0)&=1-\exp\left(-\frac{\kappa^2}{\kappa_0^2}\right),\end{aligned}\tag{7}$$

where z is the propagation distance, $\kappa_X(\alpha)$ and $\kappa_Y(\alpha)$ represent cut-off spatial frequencies, $\Lambda=\Lambda_0/\left(\Theta_0^2+\Lambda_0^2\right)$ is the output plane beam parameter that is related to the input plane beam parameters $\Lambda_0=2L/\left(kW_0^2\right)$ and $\Theta_0=1-L/F_0$, F_0 and W_0 denote the phase front radius of curvature and the beam radius at the transmitter, respectively. The remaining parameters κ_0 and κ_l are defined by $\kappa_0=8\pi/L_0$ and, $\kappa_l=c(\alpha)/l_0$, respectively, with

$$\begin{aligned}c(\alpha) &= \left\{\pi A(\alpha)\left[\Gamma\left(\frac{3-\alpha}{2}\right)\left(\frac{3-\alpha}{3}\right)\right.\right.\\ &\quad\left.\left.+a_1\Gamma\left(2-\frac{\alpha}{2}\right)\left(\frac{4-\alpha}{3}\right)\right.\right.\end{aligned}$$

$$-b_1\Gamma\left(\frac{3-\alpha+\beta}{2}\right)\left(\frac{3-\alpha+\beta}{3}\right)\Bigg]\Bigg\}^{1/(\alpha-5)}. \quad (8)$$

The values of the parameters a_1, b_1, and β in Eqs. (7) and (8) depend on further experimental results.

3. Scintillation index for Gaussian-beam wave with inner- and outer-scale effects

The SI for a Gaussian-beam wave propagating through weak non-Kolmogorov atmospheric turbulence is given by[3]

$$\sigma_I^2(\alpha,r,L)=\sigma_{I,r}^2(\alpha,r,L)+\sigma_{I,l}^2(\alpha,L), \quad (9)$$

where

$$\sigma_{I,r}^2(\alpha,r,L) = 8\pi^2k^2L\int_0^1\int_0^\infty \kappa\Phi_n(\kappa,\alpha)\exp\left(-\frac{\Lambda L\kappa^2\xi^2}{k}\right) \times\left[I_0(2\Lambda r\xi k)-1\right]\mathrm{d}\kappa\mathrm{d}\xi, \quad (10)$$

$$\sigma_{I,l}^2(\alpha,L) = 8\pi^2k^2L\int_0^1\int_0^\infty \kappa\Phi_n(\kappa,\alpha)\exp\left(-\frac{\Lambda L\kappa^2\xi^2}{k}\right) \times\left\{1-\cos\left[\frac{L\kappa^2}{k}\xi\left(1-\bar{\Theta}\xi\right)\right]\right\}\mathrm{d}\kappa\mathrm{d}\xi, \quad (11)$$

where $\xi=1-z/L$ is the normalized distance variable, $\bar{\Theta}=1-\Theta$ is the complementary parameter, $\Theta=\Theta_0/\left(\Theta_0^2+\Lambda_0^2\right)$ is the output plane beam parameter that is related to the input plane beam parameters, $I_0(\cdot)$ is a modified Bessel function of the first kind, r is the distance from the beam center line in the plane transverse to the propagation distance, $\sigma_{I,r}^2(\alpha,r,L)$ is called the radial component of the scintillation index (RSI) that describes the off-axis contribution to the SI, whereas the longitudinal component of the scintillation index (LSI) $\sigma_{I,l}^2(\alpha,L)$ corresponds to the on-axis SI.

3.1. Scintillation index for saturation regime non-Kolmogorov turbulence

According to the asymptotic theory, when the inner scale is taken into account in the saturation regime, the SI for a Gaussian-beam wave based on the generalized modified atmospheric spectrum can be expressed as[3]

$$\sigma_{I,R}^2(\alpha,L) = 1+32\pi^2k^2L\int_0^1\int_0^\infty \kappa\Phi_n(\kappa,\alpha)f(\kappa,\alpha,l_0) \times\exp\left(-\frac{\Lambda L\kappa^2\xi^2}{k}\right)\sin^2\left[\frac{L\kappa^2}{2k}\xi\left(1-\bar{\Theta}\xi\right)\right] \times\exp\left\{-\int_0^1 D_s\left[\frac{L\kappa}{k}w(\tau,\xi)\right]\mathrm{d}\tau\right\}\mathrm{d}\kappa\mathrm{d}\xi, \quad \tilde{\sigma}_R^2(\alpha)\gg 1, \quad (12)$$

where τ is a normalized distance variable, and the exponential function acts like a low-pass spatial filter defined by the phase structure function (PSF) for a plane wave $D_s(\rho,\alpha)$. The function $w(\tau,\xi)$ is defined by

$$w(\tau,\xi)=\begin{cases}\tau\left(1-\bar{\Theta}\xi\right), \tau<\xi,\\ \xi\left(1-\bar{\Theta}\tau\right), \tau>\xi.\end{cases} \quad (13)$$

When the separation distance ρ is smaller than the inner scale of turbulence l_0, then based on the generalized modified atmospheric spectrum, the PSF for a plane wave $D_s(\rho,\alpha)$ is given (see Appendix A).

$$D_s(\rho,\alpha) = 0.5\pi^2A(\alpha)h(\alpha)\Xi(\alpha)C_n^2k^2L \times[c(\alpha)]^{4-\alpha}l_0^{\alpha-4}\rho^2, \quad (14)$$

where

$$\Xi(\alpha) = \Gamma\left(1-\frac{\alpha}{2}\right)\left(1-\frac{\alpha}{2}\right)+a_1\Gamma\left(\frac{3-\alpha}{2}\right)\left(\frac{3-\alpha}{2}\right) -b_1\Gamma\left(1+\frac{\beta-\alpha}{2}\right)\left(1+\frac{\beta-\alpha}{2}\right). \quad (15)$$

Substituting Eqs. (13) and (14) into Eq. (12), we obtain

$$\int_0^1 D_s\left[\frac{L\kappa}{k}w(\tau,\xi)\right]\mathrm{d}\tau = \frac{\tilde{\sigma}_R^2(\alpha)\Xi(\alpha)}{2g_1(\alpha)}[Q_l(\alpha)]^{2-\frac{\alpha}{2}}\left(\frac{L\kappa^2}{k}\right)\xi^2 \times\left(1-\bar{\Theta}+\frac{\bar{\Theta}^2}{3}-\frac{2\xi}{3}+\frac{\bar{\Theta}\xi^2}{3}\right), \quad (16)$$

where $Q_l(\alpha)=[c(\alpha)]^2L/\left(kl_0^2\right)$,

$$\tilde{\sigma}_R^2(\alpha)=g_1(\alpha)\pi^2A(\alpha)h(\alpha)C_n^2k^{3-\alpha/2}L^{\alpha/2}$$

is the non-Kolmogorov Rytov variance for a plane wave under weak turbulence,[30] and $g_1(\alpha)=4\Gamma(-\alpha/2)\sin(\pi\alpha/4)$. Under the geometrical optical approximation, we have

$$\sin^2\left[\frac{L\kappa^2}{2k}\xi\left(1-\bar{\Theta}\xi\right)\right]\cong\frac{L^2\kappa^4}{4k^2}\xi^2\left(1-\bar{\Theta}\xi\right)^2, \quad \exp\left(-\frac{\Lambda L\kappa^2\xi^2}{k}\right)\cong 1, \quad (17)$$

then substituting Eqs. (16) and (17) into Eq. (12), the analytical expressions of $\sigma_{I,R}^2(\alpha,L)$ for a Gaussian-beam wave is obtained as

$$\sigma_{I,R}^2(\alpha,L)=1+\frac{C_G(\alpha)}{\left\{\tilde{\sigma}_R^2(\alpha)[Q_l(\alpha)]^{3-\alpha/2}\right\}^{2-\alpha/2}}, \quad (18)$$

where

$$C_G(\alpha) = \frac{4\Gamma(3-\alpha/2)}{g_1(\alpha)}\left\{\tilde{\sigma}_R^2(\alpha)[Q_l(\alpha)]^{3-\alpha/2}\right\}^{3-\alpha/2} \times\left[Z(\alpha,0)+a_1Z(\alpha,1/2)-b_1Z(\alpha,\beta/2)\right], \quad (19)$$

with

$$Z(\alpha,v)=\int_0^1 \frac{\Gamma\left(3-\frac{\alpha}{2}+v\right)\left[\Gamma\left(3-\frac{\alpha}{2}\right)\right]^{-1}\xi^2\left(1-\bar{\Theta}\xi\right)^2}{\left[1+\frac{\tilde{\sigma}_R^2(\alpha)\Xi(\alpha)}{2g_1(\alpha)}\left[Q_l(\alpha)\right]^{3-\frac{\alpha}{2}}\xi^2\left(1-\bar{\Theta}+\frac{\bar{\Theta}^2}{3}-\frac{2\xi}{3}+\frac{\bar{\Theta}\xi^2}{3}\right)\right]^{v+3-\alpha/2}}\mathrm{d}\xi. \tag{20}$$

When $\bar{\Theta}=0$, equation (18) reduces to the plane wave SI in the saturation regime, or the spherical wave SI in the saturation regime when $\bar{\Theta}=1$.

3.2. Longitudinal component of the scintillation index

When the inner scale and outer scale effects are taken into account, under moderate-to-strong non-Kolmogorov turbulence, by using the extended Rytov theory, the LSI takes the following form:

$$\sigma_{I,l}^2(\alpha,L)=\exp\left[\sigma_{l,\ln X}^2(\alpha,l_0)-\sigma_{l,\ln X}^2(\alpha,L_0)+\sigma_{l,\ln Y}^2(\alpha,l_0)\right]-1, \tag{21}$$

where $\sigma_{l,\ln X}^2(\alpha,l_0)$ and $\sigma_{l,\ln X}^2(\alpha,L_0)$ are the large-scale log-irradiance variance under the presence of finite inner scale and finite outer scale, respectively, and $\sigma_{l,\ln Y}^2(\alpha,l_0)$ is the small-scale log-irradiance variance.

In the presence of a finite inner scale, the large-scale log-irradiance variance for a beam wave is given by[3]

$$\begin{aligned}&\sigma_{l,\ln X}^2(\alpha,l_0)\\&=8\pi^2k^2L\int_0^1\int_0^\infty \kappa\Phi_n(\kappa,\alpha)G_X(\kappa,\alpha,l_0)\exp\left(-\frac{\Lambda L\kappa^2\xi^2}{k}\right)\\&\times\left\{1-\cos\left[\frac{L\kappa^2}{k}\xi\left(1-\bar{\Theta}\xi\right)\right]\right\}\mathrm{d}\kappa\mathrm{d}\xi.\end{aligned} \tag{22}$$

Based on the change of parameters $\eta=L\kappa^2/k$, $\eta_X(\alpha)=L\kappa_X^2(\alpha)/k$, and using the geometrical optical approximation (Eq. (17)), equation (22) reduces to

$$\begin{aligned}&\sigma_{l,\ln X}^2(\alpha,l_0)\\&\cong\frac{2\tilde{\sigma}_R^2(\alpha)}{g_1(\alpha)}\int_0^1\xi(1-\xi)^2\int_0^\infty\eta^{2-\alpha/2}\\&\times\exp\left[-\eta/Q_l(\alpha)-\eta/\eta_X(\alpha)\right]\\&\times\left[1+a_1\left(\frac{\eta}{Q_l(\alpha)}\right)^{1/2}-b_1\left(\frac{\eta}{Q_l(\alpha)}\right)^{\beta/2}\right]\mathrm{d}\eta\,\mathrm{d}\xi.\end{aligned} \tag{23}$$

Upon evaluation of the integral, we obtain

$$\begin{aligned}&\sigma_{l,\ln X}^2(\alpha,l_0)\\&=\frac{2\Gamma(3-\alpha/2)\tilde{\sigma}_R^2(\alpha)}{g_1(\alpha)}\left(\frac{1}{3}-\frac{\bar{\Theta}}{2}+\frac{\bar{\Theta}^2}{5}\right)\\&\times\left(\frac{\eta_X(\alpha)Q_l(\alpha)}{\eta_X(\alpha)+Q_l(\alpha)}\right)^{3-\alpha/2}\\&\times\left\{1+a_1\frac{\Gamma[(7-\alpha)/2]}{\Gamma(3-\alpha/2)}\left(\frac{\eta_X(\alpha)}{\eta_X(\alpha)+Q_l(\alpha)}\right)^{1/2}\right.\\&\left.-b_1\frac{\Gamma[3+(\beta-\alpha)/2]}{\Gamma(3-\alpha/2)}\left(\frac{\eta_X(\alpha)}{\eta_X(\alpha)+Q_l(\alpha)}\right)^{\beta/2}\right\}.\end{aligned} \tag{24}$$

Similarly, the large-scale log-irradiance variance with outer scale effect can be expressed as

$$\begin{aligned}&\sigma_{l,\ln X}^2(\alpha,L_0)\\&=\frac{2\Gamma(3-\alpha/2)\tilde{\sigma}_R^2(\alpha)}{g_1(\alpha)}\left(\frac{1}{3}-\frac{\bar{\Theta}}{2}+\frac{\bar{\Theta}^2}{5}\right)\\&\times\left(\frac{\eta_{X0}(\alpha)Q_l(\alpha)}{\eta_{X0}(\alpha)+Q_l(\alpha)}\right)^{3-\alpha/2}\\&\times\left\{1+a_1\frac{\Gamma[(7-\alpha)/2]}{\Gamma(3-\alpha/2)}\left(\frac{\eta_{X0}(\alpha)}{\eta_{X0}(\alpha)+Q_l(\alpha)}\right)^{1/2}\right.\\&\left.-b_1\frac{\Gamma[3+(\beta-\alpha)/2]}{\Gamma(3-\alpha/2)}\left(\frac{\eta_{X0}(\alpha)}{\eta_{X0}(\alpha)+Q_l(\alpha)}\right)^{\beta/2}\right\},\end{aligned} \tag{25}$$

where $\eta_{X0}(\alpha)=\eta_X(\alpha)Q_0/[\eta_X(\alpha)+Q_0]$ and $Q_0=64\pi^2L/(kL_0^2)$.

Since the form of the filter function is the same as that of the small log-irradiance scintillations in this case as well as the zero inner scale case, the corresponding log-irradiance variance of the small-scale process for a beam wave is again described by Eq. (38) in Ref. [20]

$$\sigma_{l,\ln Y}^2(\alpha,l_0)=\frac{8\tilde{\sigma}_R^2(\alpha)}{(\alpha-2)g_1(\alpha)}\eta_Y^{1-\alpha/2}(\alpha). \tag{26}$$

However, when the inner scale is taken into account, $\eta_Y(\alpha)$ is related to the SI based on the generalized modified atmospheric spectrum.

To determine the unknown parameters in Eq. (24) and in Eq. (26), using Eq. (18) and following the same procedure as discussed in Refs. [19] and [20], we obtain

$$\begin{aligned}\frac{1}{\eta_X(\alpha)}&=\left[\frac{2\Gamma(3-\alpha/2)}{0.49g_1(\alpha)}\left(\frac{1}{3}-\frac{\bar{\Theta}}{2}+\frac{\bar{\Theta}^2}{5}\right)\right]^{\frac{2}{6-\alpha}}\left(\frac{\tilde{\sigma}_R^2(\alpha)}{\tilde{\sigma}_B^2(\alpha)}\right)^{\frac{2}{6-\alpha}}\\&+\left[\frac{C_G(\alpha)g_1(\alpha)}{4\Gamma\left(3-\frac{\alpha}{2}\right)\left(\frac{1}{3}-\frac{\bar{\Theta}}{2}+\frac{\bar{\Theta}^2}{5}\right)}\right]^{\frac{2}{\alpha-6}}\\&\times\tilde{\sigma}_R^2(\alpha)Q_l(\alpha)^{2-\frac{\alpha}{2}},\end{aligned} \tag{27}$$

$$\begin{aligned}\eta_Y(\alpha)&=\left[\frac{0.51(\alpha-2)g_1(\alpha)}{8}\right]^{\frac{2}{2-\alpha}}\left(\frac{\tilde{\sigma}_G^2(\alpha)}{\tilde{\sigma}_R^2(\alpha)}\right)^{\frac{2}{2-\alpha}}\\&\times\left[1+\left(\frac{\ln 2}{0.51}\right)^{\frac{2}{2-\alpha}}\tilde{\sigma}_G^{\frac{4}{\alpha-2}}(\alpha)\right],\end{aligned} \tag{28}$$

where $\tilde{\sigma}_B^2(\alpha)$ and $\tilde{\sigma}_G^2(\alpha)$ are the LSI for a Gaussian-beam wave based on the generalized Kolmogorov spectrum[22] and

the generalized modified atmospheric spectrum,[24] respectively.

Therefore, substituting Eq. (27) into Eqs. (24) and (25), and inserting Eq. (28) into Eq. (26), the LSI for a Gaussian-beam wave in moderate-to-strong non-Kolmogorov turbulence can be obtained as

$$\sigma_{I,l}^2(\alpha,L) = \exp\left\{\sigma_{l,\ln X}^2(\alpha,l_0)-\sigma_{l,\ln X}^2(\alpha,L_0) + \frac{0.51\tilde{\sigma}_G^2(\alpha)}{\left[1+\left(\frac{\ln 2}{0.51}\right)^{\frac{2}{2-\alpha}}\tilde{\sigma}_G^{\frac{4}{\alpha-2}}(\alpha)\right]^{\alpha/2-1}}\right\}-1. \quad (29)$$

3.3. Radial component of the scintillation index

As pointed out in Section 9.6.3 in Ref. [3], the RSI is relatively insensitive to the effects of the inner scale. Therefore, we will include the outer scale effects only for the RSI. Based on the outer scale model for this parameter as given in Ref. [3] and using the method of effective beam parameters, the RSI of a Gaussian-beam wave under weak-to-strong non-Kolmogorov turbulence can be approximated as follows:

$$\sigma_{I,r}^2(\alpha,r,L) = \frac{8\tilde{\sigma}_R^2(\alpha)\Gamma(2-\alpha/2)}{g_1(\alpha)(\alpha-1)} \times\left[1+\frac{\Gamma(\alpha/2-2)(\alpha-1)}{3\Gamma(\alpha/2)\Gamma(2-\alpha/2)}\left(\frac{\Lambda_e L}{kL_0^2}\right)^{2-\frac{\alpha}{2}}\right]\Lambda_e^{\frac{\alpha}{2}-1}\frac{r^2}{W_{LT}^2}, \quad 0\le r<W, \quad (30)$$

where the effective beam parameters Λ_e and W_{LT} are defined by[31]

$$\Lambda_e=\frac{2L}{kW_{LT}^2}=\frac{\Lambda}{1+4q\Lambda/3}, \quad W_{LT}=W\sqrt{1+4q\Lambda/3}, \quad (31)$$

with $q=L/\left[k\rho_p^2(\alpha)\right]$, where $\rho_p(\alpha)$ is the coherence length of a plane wave. For non-Kolmogorov turbulence, $\rho_p(\alpha)$ is given by[32]

$$\rho_p(\alpha)=\left[-\frac{2^{3-\alpha}\Gamma(1-\alpha/2)}{\Gamma(\alpha/2)}A(\alpha)h(\alpha)C_n^2\pi^2k^2L\right]^{-\frac{1}{\alpha-2}}. \quad (32)$$

As $\alpha=11/3$, equation (30) reduces to the RSI (Eq. (62) in Ref. [4]) in the conventional Kolmogorov turbulence.

3.4. Scintillation index for Gaussian-beam wave

For moderate-to-strong non-Kolmogorov turbulence, by combining the longitudinal component Eq. (29) and the radial component Eq. (30), the SI for a Gaussian-beam wave with the inner scale and outer scale effects can be represented as

$$\sigma_I^2(\alpha,r,L) = \frac{8\tilde{\sigma}_R^2(\alpha)\Gamma(2-\alpha/2)}{g_1(\alpha)(\alpha-1)} \times\left[1+\frac{\Gamma(\alpha/2-2)(\alpha-1)}{3\Gamma(\alpha/2)\Gamma(2-\alpha/2)}\left(\frac{\Lambda_e L}{kL_0^2}\right)^{2-\frac{\alpha}{2}}\right]\Lambda_e^{\frac{\alpha}{2}-1}\frac{r^2}{W_{LT}^2} + \exp\left\{\sigma_{l,\ln X}^2(\alpha,l_0)-\sigma_{l,\ln X}^2(\alpha,L_0) + \frac{0.51\tilde{\sigma}_G^2}{\left[1+\left(\frac{\ln 2}{0.51}\right)^{\frac{2}{2-\alpha}}\tilde{\sigma}_G^{\frac{4}{\alpha-2}}\right]^{\alpha/2-1}}\right\}-1, \quad 0\le r<W. \quad (33)$$

Compared with the SI for the case of zero inner scale and infinite outer scale,[20] to obtain Eq. (33), the minor modifications in both the radial and longitudinal components that might arise from beam wander pointing error effects are ignored. Therefore, the usefulness of Eq. (33) might be limited to untracked collimated or divergent beams and to convergent beams with initial beam diameters which are not too large. When $\alpha=11/3$, equation (33) reduces to the expression for Kolmogorov turbulence.[4,20]

4. Numerical results

In this section, some numerical results are presented to analyze the characteristics of the SI for a Gaussian-beam wave propagating through moderate-to-strong non-Kolmogorov turbulence obtained above, including the effects of the spectral power law α, the inner scale l_0 and outer scale L_0. Unless otherwise noted, all the results presented are based on the parameters of $\lambda=1550$ nm, $C_n^2=5\times10^{-13}$ m$^{-2/3}$, $W_0=0.01$ m, $\Theta_0=1$, and the parameters of the spectrum are set to be $a_1=1.802$, $b_1=0.254$, $\beta=7/6$.[19,24] In addition, when the parameters λ, C_n^2, α in $\tilde{\sigma}_R^2(\alpha)$ are fixed, the increase of L corresponds to the strength of the turbulence increase.

To analyze the influence of the inner and outer scale on the Gaussian-beam wave SI, in Fig. 1, we illustrate the LSI for a collimated Gaussian-beam wave from Eq. (33) with $r=0$ as a function of L, with inner scale values $l_0=2$ mm and 8 mm and outer scale values $L_0=1$ m and ∞. We set $\alpha=3.1$, 10/3, 11/3, and 3.9 in the Figs. 1(a), 1(b), 1(c), and 1(d), respectively. Regardless of the values of α, l_0, L_0, from the figure, LSI increases steeply with the initial increase of L, until it reaches a peak value in the focusing regime (location of peak LSI) where large-scale inhomogeneity achieves its strongest effect. It then decreases with an increase of L and tends to saturate at a level. This occurs because with a further increase of L, the focus effect is weakened by multiple scattering. Then in the saturation regime, the multiple scattering leads to optical wavelike extended multiple sources, and causes each source to scintillate with a distinct random phase. Also, for different l_0, L_0 and α, the peak LSI has various values and occurs at different L. This is because under strong fluctuations, the SI is associated with three critical turbulence cell sizes which include the spatial coherence radius, the scattering disk radius

and L_0. Besides, the spatial coherence radius (ρ_0, Eq. (A13)) and the scattering disk ($L/(k\rho_0)$) depend on the l_0 and α.

In addition, we noted that for some fixed α, the outer scale has a negligible effect on the LSI for short path lengths, which corresponds to weak fluctuations. However, when $L >$ 2 km the presence of a finite outer scale starts to reduce the LSI at a steeper rate compared to the case of an infinite outer scale, and the rate of reduction depends on l_0 and α. This observation is similar to that for the plane and spherical waves in a previous report.[15] We also note that in the saturation regime, for a fixed inner scale value, the gap of LSI between the finite outer scale and the infinite outer scale increases with increasing α. This indicates that for a larger α, the effects of the outer scale on the LSI cannot be ignored over long distance FSO communication. Moreover, for any α, the presence of an inner scale does not significantly influence the LSI under weak fluctuations. Under moderate-to-strong fluctuations, larger inner scale value leads to stronger LSI, and a significant increase occurs near the focusing regime. In particular, the gap of the LSI near the focusing regime between the larger inner scale value ($l_0 = 8$ mm) and the smaller inner scale value ($l_0 = 2$ mm) is the largest for $\alpha = 10/3$ and is smallest for $\alpha = 3.9$. This occurs because the inner scale plays a role in defining the scattering disk, and the difference of the scattering disk between $l_0 = 8$ mm and $l_0 = 2$ mm for $\alpha = 10/3$ is larger than that for $\alpha = 3.9$. In addition, the difference of the LSI between the larger inner scale and the smaller inner scale decreases with increasing path length, which means that the influence of the inner scale tends to diminish with increasing turbulence strength, especially in the presence of a finite outer scale case. For instance, when $L > 8$ km and $L_0 = 1$ m, the influence of the inner scale can be considered negligible.

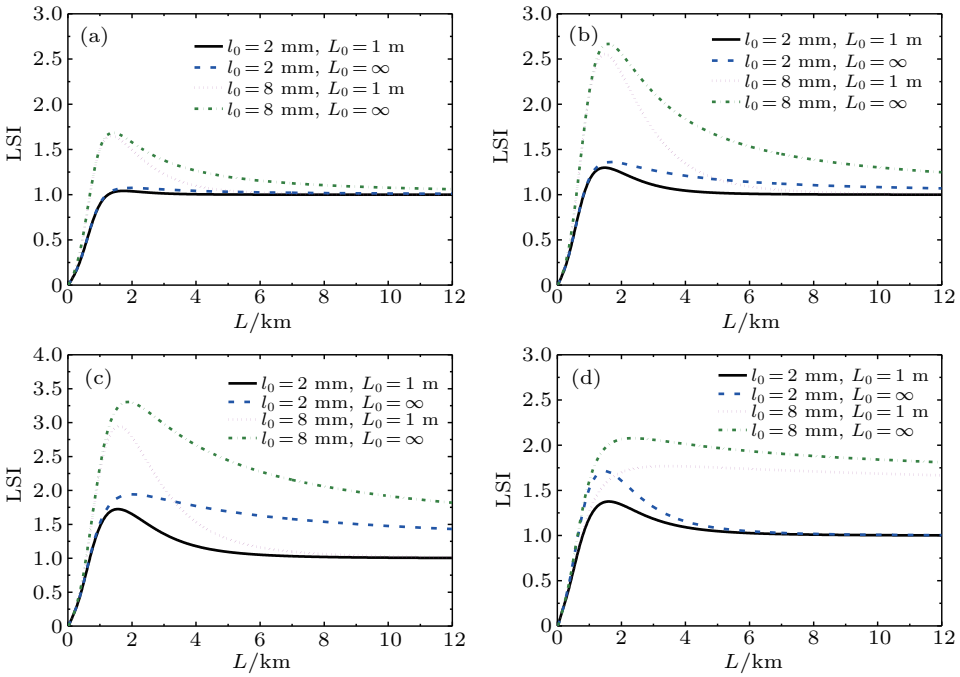


Fig. 1. (color online) Longitudinal component of the SI (LSI) of a Gaussian-beam wave as a function of L for different l_0 and L_0 values. (a) $\alpha = 3.1$, (b) $\alpha = 10/3$, (c) $\alpha = 11/3$, (d) $\alpha = 3.9$.

Figure 2 shows the LSI for a collimated Gaussian-beam wave as a function of α, for inner scale values $l_0 = 2$ mm and 8 mm. In this case, the outer scale parameter is set at $L_0 = \infty$. Another group of curves is obtained using the same parameters except $L_0 = 1$ m, as comparable LSI values. Regardless of the values of L, l_0, L_0, as shown in Fig. 2, the LSI increases with increasing α up to peak values, then the LSI decreases rapidly as α approaches value 4. The peak values of the LSI for different L, l_0, and L_0 have various values and occur at different α, especially for the larger L cases which correspond to the stronger fluctuation conditions. In Fig. 2(a), we set the path length $L = 200$ m, which corresponds to weak fluctuation conditions. As shown, for a fixed inner scale value, the curves with $L_0 = 1$ m almost coincides with the curves for $L_0 = \infty$. This means that the outer scale has no noticeable effect on the LSI under weak fluctuations, for all values of α. This is consistent with weak fluctuation theory as previously reported.[23] As for the inner scale effects, we noted that the larger inner scale value ($l_0 = 8$ mm) results in a larger LSI, except for α close to 4. This can be explained by considering the behavior of the generalized effective atmospheric spectrum. In Fig. 2(b), the path length L is set to 1000 m, which corresponds to stronger fluctuation conditions. We clearly observe that when $3.2 < \alpha < 4$ the gap of the LSI between the finite outer scale case and the infinite outer scale case begins to increase, meaning that the finite outer scale begins to re-

duce the LSI. For a fixed given L_0, the LSI with $l_0 = 8$ mm is significantly larger than with $l_0 = 2$ mm, except when α is close to 3 and 4. In Fig. 2(c), we set $L = 2000$ m. We deduce that for a fixed inner scale value, the finite outer scale results in a greater reduction of the LSI compared with that in Fig. 2(b). This implies that the effects of the outer scale on the LSI becomes stronger with the increasing strength of the turbulence. Moreover, the gap of the LSI between $l_0 = 8$ mm and $l_0 = 2$ mm tends to decrease, especially for finite outer cases. This indicates that the influence of the inner scale on the LSI decreases with an increase of the turbulence strength. In Fig. 2(d), the path length was set at $L = 6000$ m. Under this extremely strong turbulence conditions, we noted that for both the larger inner scale and smaller inner scale cases, the finite outer scale significantly reduces the LSI except at both ends of the α range. In addition, for the fixed inner scale, the gap of the LSI between the finite outer scale case and the infinite outer scale case increases compared with that in Fig. 2(c). This implies that the outer scale effects cannot be ignored under extremely strong turbulence conditions, especially for the cases with a larger spectral power law. In addition, the inner scale has no appreciable effect on the LSI for the cases with $L_0 = 1$ m, whereas when $L_0 = \infty$, the effects of the inner scale on the LSI decreases compared with that in Fig. 2(c). It is shown that the general inner scale and outer scale behavior depicted here for a Gaussian-beam wave is basically the same for the infinite plane wave and spherical wave in a previous report[15,19] under moderate-to-strong non-Kolmogorov turbulence.

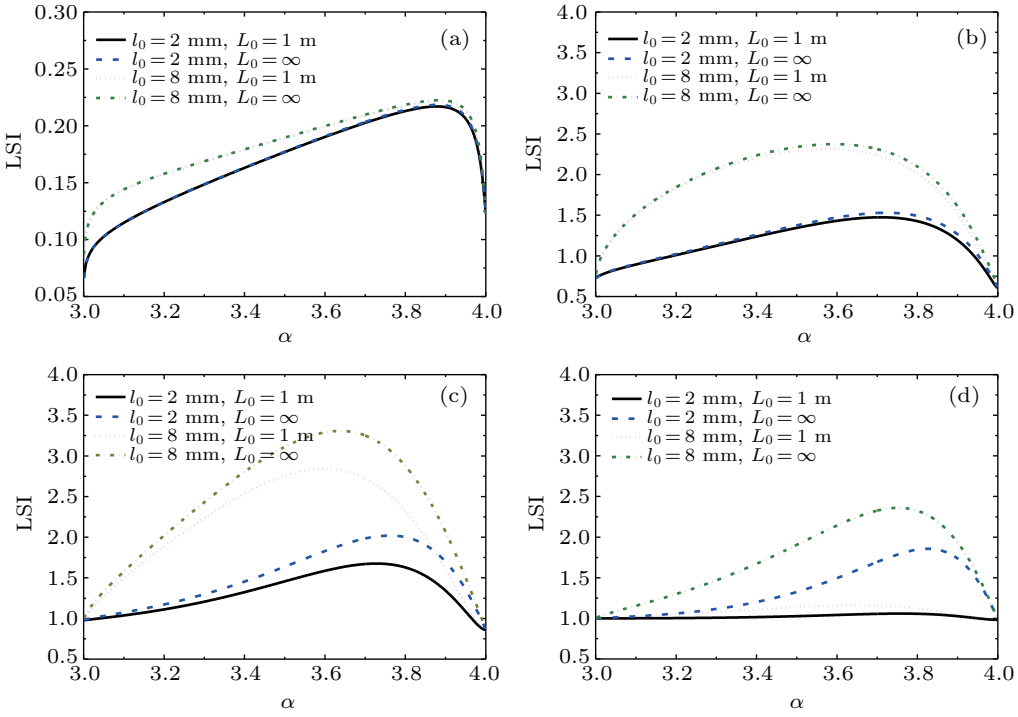


Fig. 2. (color online) Longitudinal component of the SI (LSI) of a Gaussian-beam wave as a function of α with different l_0 and L_0 values; (a) $L = 200$ m, (b) $L = 1000$ m, (c) $L = 2000$ m, (d) $L = 6000$ m.

All the conclusions above are based on the LSI for a collimated Gaussian-beam wave for $r = 0$. To further analyze the effects of the radial component on SI, we plot both on- and off-axis results deduced from Eq. (33) in Fig. 3, where we set $\alpha = 10/3$, $l_0 = 2$ mm, $L_0 = 1$ m under the conditions cited for Fig. 1(b). It is clear that the addition of the radial component results in an increase in the SI compared with the on-axis SI. This means that the off-axis fluctuations are stronger than the on-axis fluctuations. However, once the beam has passed through the focusing regime, the radial dependence of the SI tends to diminish. For instance, when $L > 8$ km, the radial component has no appreciable effect on the SI. In addition, as the value of r/W increases, the SI power exponent increases under weak to focusing regime fluctuation conditions.

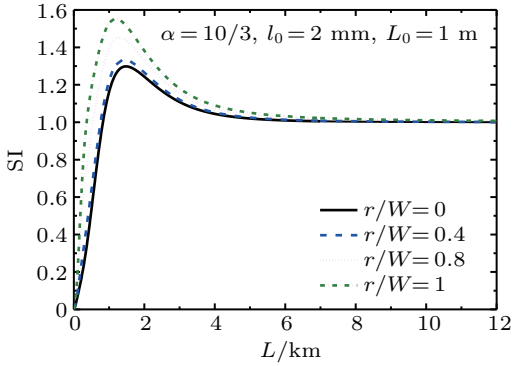


Fig. 3. (color online) SI of Gaussian-beam wave as a function of L for various values of r/W.

5. Conclusion

In this paper, we have derived a theoretical expression for the SI of a Gaussian-beam wave propagating through moderate-to-strong non-Kolmogorov turbulence, using the generalized effective atmospheric spectrum and the extended Rytov method. The derived expression was used to analyze the effects of the spectral power law, inner scale, and outer scale on the SI.

The numerical results reveal that for moderate-to-strong non-Kolmogorov turbulence, the SI increases with increasing path length up to a peak value at the focusing regime, then decreases and tends to saturate at a level. For different l_0, L_0, and α, the peak SI has various values and occurs at different L. Moreover, the SI power exponent increases under weak to focusing regime fluctuation conditions with increasing r/W. For outer scale effects, it has a negligible effect on the longitudinal component of the SI under weak fluctuation. However, for all values of α and larger path lengths, it reduces the SI at a steeper rate compared to the SI for an infinite outer scale, and the rate of reduction depends on l_0 and α. In addition, the presence of an inner scale does not significantly influence the SI under weak fluctuations. However, under moderate-to-strong fluctuations, larger inner scale values lead to stronger SI and a significant increase occurs near the focusing regime. The influence of the inner scale on the SI tends to diminish with increasing turbulence strength. These results will contribute to further investigations and the understanding of optical wave propagation in the atmospheric turbulence.

Appendix A

In this appendix, the expression of the phase structure function (PSF) for a plane wave based on the generalized modified atmospheric spectrum for the case $L_0 = \infty$ is derived.

The plane wave structure function (WSF) is given by[3]

$$D_{pl}(\alpha,\rho) = 8\pi^2 k^2 L \int_0^\infty \kappa \Phi_n(\kappa,\alpha) f(\kappa,\alpha,l_0) \times [1 - J_0(\kappa\rho)]\,\mathrm{d}\kappa. \tag{A1}$$

Substituting Eqs. (2), (3) and (7) into Eq. (A1), we obtain

$$D_{pl}(\alpha,\rho) = 8\pi^2 A(\alpha) h(\alpha) C_n^2 k^2 L \int_0^\infty \kappa^{1-\alpha} [1 - J_0(\kappa\rho)] \times \left[1 + a_1\left(\frac{\kappa}{\kappa_l}\right) - b_1\left(\frac{\kappa}{\kappa_l}\right)^\beta\right] \exp\left(\frac{\kappa^2}{\kappa_l^2}\right) \mathrm{d}\kappa. \tag{A2}$$

Using the series representation of the Bessel function of the first kind,[3]

$$J_0(x) = \sum_{n=0}^\infty \frac{(-1)^n (x/2)^{2n+p}}{n!\Gamma(n+p+1)}, \quad |x| < \infty, \tag{A3}$$

equation (A2) can be re-expressed as

$$D_{pl}(\alpha,\rho) = 8\pi^2 A(\alpha) h(\alpha) C_n^2 k^2 L \sum_{n=1}^\infty \frac{(-1)^{n-1} (\rho/2)^{2n}}{n!\Gamma(n+1)} \times \int_0^\infty \kappa^{2n+1-\alpha} \left[1 + a_1\left(\frac{\kappa}{\kappa_l}\right) - b_1\left(\frac{\kappa}{\kappa_l}\right)^\beta\right] \times \exp\left(\frac{\kappa^2}{\kappa_l^2}\right) \mathrm{d}\kappa, \tag{A4}$$

and then using the definition of Gamma function $\Gamma(\cdot)$ and hypergeometric ${}_1\mathrm{F}_1(\cdot)$,[3]

$$\Gamma(x) = \int_0^\infty \kappa^{x-1} \exp(-\kappa)\,\mathrm{d}\kappa, \quad (\kappa > 0, x > 0), \tag{A5}$$

$${}_1\mathrm{F}_1(a;\mathrm{b};z) = \sum_{n=0}^\infty \frac{(a)_n z^n}{(b)_n n!}, \tag{A6}$$

the analytical expression of $D_{pl}(\alpha,\rho)$ is obtained.

$$\begin{aligned} &D_{pl}(\alpha,\rho) \\ &= 4\pi^2 A(\alpha) h(\alpha) C_n^2 k^2 L \kappa_l^{2-\alpha} \left\{\Gamma\left(1 - \frac{\alpha}{2}\right) \times \left[1 - {}_1\mathrm{F}_1\left(1 - \frac{\alpha}{2}; 1; -\frac{\rho^2\kappa_l^2}{4}\right)\right] \right. \\ &+ a_1\Gamma\left(1 - \frac{\alpha-1}{2}\right)\left[1 - {}_1\mathrm{F}_1\left(1 - \frac{\alpha-1}{2}; 1; -\frac{\rho^2\kappa_l^2}{4}\right)\right] \\ &\left. - b_1\Gamma\left(1 - \frac{\alpha-\beta}{2}\right)\left[1 - {}_1\mathrm{F}_1\left(1 - \frac{\alpha-\beta}{2}; 1; -\frac{\rho^2\kappa_l^2}{4}\right)\right]\right\}. \end{aligned} \tag{A7}$$

For ease of calculation, the following approximation is adopted as previously reported[33]

$$1 - {}_1\mathrm{F}_1\left(1 - \frac{\alpha}{2}; 1; -x\right) \approx \left(1 - \frac{\alpha}{2}\right) x \left\{1 + \frac{2}{(\alpha-2)\Gamma(\alpha/2)} x\right\}^{\alpha/2-2}. \tag{A8}$$

Hence, equation (A7) can be expressed as

$$D_{pl}(\alpha,\rho) = \pi^2 A(\alpha) h(\alpha) C_n^2 k^2 L [c(\alpha)]^{4-\alpha} l_0^{\alpha-4} \rho^2 \times [\Delta(\rho,\alpha) + a_1\Delta(\rho,\alpha-1) - b_1\Delta(\rho,\alpha-\beta)], \tag{A9}$$

with

$$\Delta(\rho,x) = \Gamma\left(1 - \frac{x}{2}\right)\left(1 - \frac{x}{2}\right) \times \left\{1 + \left[\frac{2}{(x-2)\Gamma(x/2)}\right]^{2/(x-4)} \frac{\rho^2 [c(\alpha)]^2}{4 l_0^2}\right\}^{x/2-2}. \tag{A10}$$

When $\rho \ll l_0$, equation (A9) reduces to

$$D_{pl}(\alpha,\rho) = \pi^2 A(\alpha) h(\alpha) \Xi(\alpha) C_n^2 k^2 L [c(\alpha)]^{4-\alpha} l_0^{\alpha-4} \rho^2, \tag{A11}$$

with

$$\Xi(\alpha)=\Gamma\left(1-\frac{\alpha}{2}\right)\left(1-\frac{\alpha}{2}\right)+a_1\Gamma\left(\frac{3-\alpha}{2}\right)\left(\frac{3-\alpha}{2}\right)-b_1\Gamma\left(1+\frac{\beta-\alpha}{2}\right)\left(1+\frac{\beta-\alpha}{2}\right). \quad \text{(A12)}$$

By setting $D_{pl}(\alpha,\rho)=2$, the implied plane wave spatial coherence radius for the case $L_0=\infty$, is

$$\rho_0(\alpha,l_0)=\left\{0.5\pi^2A(\alpha)\Xi(\alpha)h(\alpha)C_n^2k^2L\times[c(\alpha)]^{4-\alpha}l_0^{\alpha-4}\rho^2\right\}^{-1/2}. \quad \text{(A13)}$$

Moreover, for $\rho\ll l_0$ the PSF is equal to one half the WSF.[34] Hence, the analytical expression of the plane wave PSF is obtained as

$$D_s=0.5\pi^2A(\alpha)\Xi(\alpha)h(\alpha)C_n^2k^2L[c(\alpha)]^{4-\alpha}l_0^{\alpha-4}\rho^2, \quad \text{(A14)}$$

when $\alpha=11/3$, equation (A14) reduces to $D_s=1.89C_n^2k^2Ll_0^{-1/3}\rho^2$ which agrees with the result based on the conventional modified atmospheric spectrum.[5] However, the minor difference is that equation (A14) contains the term $c(\alpha)$.

Note that we used the method in a previous report[3] to derive the PSF through WSF, which is different from the results of another previous report.[19] The reason for this is that the SI obtained using Eq. (A14) matches better with the experimental and simulation results (Sections 9.5.3 and 9.6.4 in Ref. [3]) than Eq. (A10) in Ref. [19].

References

[1] Kedar D and Arnon S 2004 *IEEE Commun. Mag.* **42** S2
[2] Arnon S, Barry J, Karagiannidis G, Schober R and Uysal M 2012 *Advanced Optical Wireless Communication Systems* (New York: Cambridge university press)
[3] Andrews L C and Phillips R L 2005 *Laser beam propagation through random media* (Bellingham, Washington: SPIE press)
[4] Andrews L C, Al-Habash M, Hopen C and Phillips R 2001 *Waves in Random Media* **11** 271
[5] Andrews L C, Phillips R L, Hopen C Y and Al-Habash M 1999 *J. Opt. Soc. Am. A* **16** 1417
[6] Rao R Z 2009 *Chin. Phys. B* **18** 581
[7] Li Y Q, Wu Z S, Zhang Y Y and Wang M J 2014 *Chin. Phys. B* **23** 74202
[8] Belen'kii M S, Cuellar E, Hughes K A and Rye V A 2006 *SPIE Optics Photonics*, p. 63040U-1
[9] Kyrazis D T, Wissler J B, Keating D D, Preble A J and Bishop K P 1994 *OE/LASE'94*, p. 43
[10] Zilberman A, Golbralkh E, Kopeika N S, Virtser A, Kupershmidt I and Shtemler Y 2008 *Atmos. Res.* **88** 66
[11] Elperin T, Kleeorin N and Rogachevskii I I 1996 *Phys. Rev. E* **53** 3431
[12] Golbraikh E and Kopeika N S 2004 *Appl. Opt.* **43** 6151
[13] Toselli I, Andrews L C, Phillips R L and Ferrero V 2007 *Lasers and Applications in Science and Engineering*, p. 64570T-1
[14] Toselli I, Andrews L C, Phillips R L and Ferrero V 2007 *Defense and Security Symposium*, p. 65510E
[15] Yi X, Liu Z J and Yue P 2012 *Opt. Express* **20** 4232
[16] Xue B D, Cui L Y, Xue W F, Bai X Z and Zhou F G 2011 *J. Opt. Soc. Am. A* **28** 912
[17] Cui L Y, Xue B D, Zheng S L, Xue W F, Bai X Z, Cao X G and Zhou F G 2012 *J. Opt. Soc. Am. A* **29** 1091
[18] Toselli I, Andrews L C, Phillips R L and Ferrero V 2007 *Remote Sensing*, p. 67470B-1
[19] Yi X, Liu Z J and Yue P 2013 *Opt. Laser Technol.* **47** 199
[20] Deng P, Yuan X H and Huang D X 2012 *Opt. Commun.* **285** 880
[21] Toselli I, Andrews L C, Phillips R L and Ferrero V 2009 *IEEE Trans. Antennas Propag.* **57** 1783
[22] Tan L Y, Du W H, Ma J, Yu S Y and Han Q Q 2010 *Opt. Express* **18** 451
[23] Cui L Y, Xue B D, Cao L, Zheng S L, Xue W F, Bai X Z, Cao X G and Zhou F G 2011 *Opt. Express* **19** 16872
[24] Cang J and Liu X 2011 *Opt. Express* **19** 19067
[25] Cang J and Liu X 2011 *Opt. Lett.* **36** 3335
[26] Champagne F, Friehe C, LaRue J and Wynagaard J 1977 *J. Aeronaut Sci.* **34** 515
[27] M W R and A P C 1977 *J. Fluid Mech.* **83** 547
[28] Barat J 1982 *J. Aeronaut Sci.* **39** 2553
[29] Baykal Y and Gerçekcioğlu H 2011 *Opt. Lett.* **36** 4554
[30] Cui L Y, Xue B D, Zheng S L, Xue W F, Bai X Z, Cao X G and Zhou F G 2012 *J. Opt. Soc. Am. A* **29**
[31] Andrews L, Miller W and Ricklin J 1994 *J. Opt. Soc. Am. A* **11** 1653
[32] Stribling B E, Welsh B M and Roggemann M C 1995 *Proc. SPIE*, p. 181
[33] Cui L Y and Xue B D 2015 *Infrared Phys. Technol.* **72** 229
[34] Andrews L C, Phillips R L and Hopen C Y 2001 *Laser Beam Scintillation with Applications* (Bellingham, Washington: SPIE press)